NASA Technical Memorandum 100931

A High Heat Flux Experiment for Verification of Thermostructural Analysis

Herbert J. Gladden and Matthew E. Melis
Lewis Research Center
Cleveland, Ohio

Prepared for the
1988 Winter Annual Meeting
of the American Society of Mechanical Engineers
Chicago, Illinois, November 28—December 2, 1988

NASA

A HIGH HEAT FLUX EXPERIMENT FOR VERIFICATION OF THERMOSTRUCTURAL ANALYSIS

Herbert J. Gladden and Matthew E. Melis
National Aeronautics and Space Administration
Lewis Research Center
Cleveland, Ohio 44135

ABSTRACT

A major concern in advancing the state-of-the-art technologies for hypersonic vehicles is the development of an aeropropulsion system capable of handling the high heat fluxes during flight. The leading edges of such systems must not only tolerate the maximum heating rates, but must also minimize distortions to the flow field due to excessive blunting and/or thermal warping of the compression surface to achieve the high inlet performance required. A combined analytical and experimental research effort has been established at NASA Lewis Research Center to study the aerothermodynamic loads on actively cooled structures for hypersonic applications. To address the experimental component of this methodology a hydrogen/oxygen rocket engine has been modified to establish a high enthalpy/high heat flux environment. The facility is capable of providing heat flux levels from about 200 up to 10 000 Btu/ft^2/sec. Crossflow and parallel flow regeneratively cooled models can be tested and analyzed by using cooling fluids of water and hydrogen. In addition, various material types can be tested and compared. These material types include high thermal conductivity copper, nickel, a graphite/copper metal matrix composite, and a tungsten/copper metal matrix composite.

This report presents results of the experiment and the characteristics of the Hot Gas Test Facility. The predicted temperature results of the crossflow model are compared with the experimental data on the first monolithic specimens and are found to be in good agreement. Thermal stress analysis results are also presented.

INTRODUCTION

The high heat flux encountered by the leading edges of a hypersonic aircraft in flight imposes severe demands on the materials and structures used for these applications. The aerodynamic heating at high flight Mach numbers, including the bow-shock wave impingement on the engine cowl lip, creates the high heat flux with corresponding high surface temperatures which can exceed the melting point of most conventional metallic and potential ceramic materials available for aerospace applications today. Not only must the high heating rates be tolerated but the distortions caused by thermal warping of the structure must be kept to a minimum to achieve high inlet performance. Consequently, a need arises for the development of actively cooled leading edges, fabricated from new materials with unique active cooling concepts incorporated, which will be able to withstand these severe environmental conditions.

A combined analytical and experimental research effort has been initiated at the NASA Lewis Research Center (1) to assess the capability of actively cooled structures to tolerate the high heating rates typical of hypersonic flight. In addition, material technologies and fabrication techniques are being studied for applying advanced metal matrix and ceramic matrix composite materials technology to actively cooled structures in a high heat flux environment. Several generic, actively cooled leading edge concepts are being developed, fabricated, and tested in a hot gas facility, and results compared with analytical predictions, under a cowl lip technology program (COLT).

The COLT program uses an interdisciplinary approach to focus the structures, fluids, materials, design, and instrumentation disciplines on the problem. Two of the concepts evaluated by the COLT team, the crossflow and the parallel flow cooling schemes, are presented in this paper. Several materials, both conventional monolithic and composites, will be tested in this effort. The materials selected are oxygen free, high conductivity (OFHC) copper, nickel 200, titanium, and copper/graphite and copper/tungsten metal matrix composites. These materials are chosen in order to examine the effect of thermal conductivities on the behavior of the cowl lip under high heating rates. Experimental data for the nickel and copper crossflow specimens are presented here, with testing yet pending on titanium and the composite specimens.

The cowl lip test pieces were subjected to high heat fluxes in a hot gas facility to simulate aerodynamic heating. The test rig is capable of providing hydrogen/oxygen combustion gas products ranging in temperatures from approximately 1800 to 5600 °F and stagnation region heat fluxes up to 10 000 Btu/ft^2/sec. Both water and gaseous hydrogen were used as coolants in the crossflow cooling scheme. Other concepts will be tested by using only gaseous hydrogen.

Two- and three-dimensional heat transfer and thermal stress analyses are performed by using the MSC/NASTRAN and MARC finite element codes. All analyses are steady-state linearly elastic solutions within NASTRAN and nonlinear transient within MARC. STAN5 (2), a boundary layer heat transfer code, and HCYLLEDG (a cylinder-in-crossflow heat transfer code based on correlations found in Ref. 3) are used to predict film coefficients on the hot gas side of the test specimens. The coolant side film coefficients are determined by correlative techniques (4,5).

In this paper the operating characteristics of the Hot Gas Test Facility are presented and compared with actual flight conditions. In addition, predicted temperature results are compared with experimental data. Thermal stress analysis results are also presented.

EXPERIMENTAL APPARATUS

Hot Gas Test Facility

The Hot Gas Test Facility can provide hydrogen/oxygen combustion gases ranging in temperatures from about 1800 to 5600 °F at combustion chamber pressures of up to 65 atm. This facility can provide Reynolds number, Prandtl number, enthalpy, and heat fluxes similar to that seen during hypersonic flight. The source of the combustion gases (primarily gaseous hydrogen and water vapor) is a rocket engine combustion chamber with a cross section of 2.3 in. by 2.3 in. which is operated in short duration bursts (approx. 3 sec). The test stand and the exhaust scrubber tank inlet pipe are shown during firing in Fig. 1(a). Figure 1(b) is a view of the test specimen looking upstream. A crossflow test specimen, test specimen holders, coolant plenum, and coolant feedlines are shown mounted in the exhaust plume.

Figure 2 shows the oxygen-to-hydrogen (O/F) ratio versus the chamber pressure design envelope for the engine and propellant feed system. Testing to date has been confined to the lower left portion of this envelope with O/F ratios of 1 to 4 and a combustion chamber pressure of about 10 atm.

Currently, the combustion gases discharge to atmosphere without benefit of a convergent-divergent nozzle; the crossflow test specimens are mounted on the downstream flange of the engine exposing the model to the exhaust plume. This flow field is essentially subsonic even though the absolute velocity is of the order of 1600 m/sec. The parallel flow and impingement flow models will be tested inside a spool-piece so that higher heat flux levels can be obtained. This spool-piece will be mounted to the downstream flange of the engine. A convergent-divergent nozzle is currently being fabricated to provide aerodynamic as well as thermodynamic similarity.

Either water or gaseous hydrogen can be used as coolant for the test specimen. Water flow rates of 24 gal/min at pressures up to 20 atm are available. Gaseous hydrogen can be provided at flow rates up to 0.15 lbm/sec and pressures up to 70 atm.

Test Specimens

Two types of test specimen were chosen to initially evaluate the facilities and demonstrate the performance of various active cooling concepts. These concepts are shown in Figs. 3 and 4 as the crossflow and parallel flow test specimens. A detailed schematic of the crossflow specimen is shown in Fig. 5. The test specimen had a 0.25-in. leading edge diameter, was 1.56 in. wide by 6.0 in. long, and had eight 0.125-in.-square cooling passages. The materials that were selected for this specimen represent a broad range of thermal conductivities. The highest thermal conductivity material that was chosen was oxygen free, high conductivity (OFHC) copper with a coefficient to thermal conductivity (TC) of 215 Btu/hr/ft/°F at room temperature. Nickel 200 was the second material chosen because of its relatively high TC of 40 Btu/hr/ft/°F, good ductility, and high melting temperature. Finally, titanium-6 aluminum-4 vanadium (Ti-6Al-4V) was chosen as a low conductivity material with a TC of 6 Btu/hr/ft/°F. The metal matrix composite copper/graphite (Cu/Gr) was also chosen as a candidate material.

The second-generation specimen to be evaluated will be the parallel flow wedge-shaped concept. This type of specimen simulates a cowl leading edge and allows for the testing of a wide range of materials. A detailed schematic of the parallel flow concept is shown in Fig. 6 with pertinent dimensions. The initial parallel flow specimen is fabricated entirely out of copper. All materials tested in the crossflow design will also be tested in the parallel flow cooling scheme as well as other more exotic materials as they become available.

Instrumentation

The material temperatures of the test specimen were measured by type-K thermocouples imbedded in longitudinal grooves machined in the surfaces. Since the crossflow specimen was made in two halves, then brazed together, thermocouples were also imbedded at the center of the coolant channel ribs. Swaged 0.020-in.-diameter thermocouples described in Ref. 6 were used. Surface static pressures were also measured on the test specimen. These pressure taps were also installed in longitudinal grooves machined in the surface. Coolant inlet and exit temperatures and pressures, as well as the total mass flow rate, were also measured.

The fuel and oxidizer flow rates to the engine were measured by sonic flow orifices. These measurements and the engine combustion chamber pressure were sufficient to calculate an ideal gas stream temperature. Attempts to measure the gas stream temperature by total temperature thermocouples have been unsuccessful to date because of the high-velocity, high-temperature flow field.

Experimental Procedure

As discussed previously in this section, several material types have been selected for evaluation on the generic leading edge concepts. Once the test specimen was fabricated and instrumented it was installed in the Hot Gas Test Facility for experimental evaluation. The test procedure for this experiment was as follows. The propellent flow rates were determined to provide the desired O/F ratio and combustion chamber pressure during the firing sequence. Before the firing sequence was initiated, the coolant flow was initiated. Once the coolant flow was established the engine firing sequence was initiated and the data recorded. The firing sequence was 3.0 sec, which was determined to be sufficient to establish steady-state test conditions and temperatures in the test specimen.

Numerical Analysis

The numerical analysis of the leading edge concepts are composed of both thermal and stress predictions using the finite element method. PATRAN II is used to create the finite element mesh required for analysis with MSC/NASTRAN and MARC. The three-dimensional model of the crossflow testpiece is made up of 4760 nodes and 3294 eight-noded hexagonal elements shown in Fig. 7. This model incorporates only the section of the testpiece that is exposed to the hot gas flow during testing; hence, the dimensions of this model are about 2.0 by 1.5 by 0.25 in. Steady-state heat transfer analysis requires convective film coefficients to be assigned to both the external surface and the cooling channel surface elements of the model. STAN5 (2), a boundary layer heat transfer code developed at Stanford University, was used to calculate the convective film coefficients on the external surfaces of cowl lip configurations. The velocity distribution at the edge of the boundary layer was determined from the MTS code (7). In addition, the stagnation point and leading edge region film coefficients were determined from a "cylinder in cross-flow" correlation (3). Coolant side film coefficients are determined by correlative techniques (4,5). Film coefficient values together with ambient gas temperatures are assigned to the model by using the NASTRAN CHBDY quadrilateral element.

Thermal linear elastic stress predictions were made with NASTRAN by imposing the nodal temperature results from the aforementioned heat transfer analysis onto the same finite element model. Elastic/plastic stress analysis with MARC was performed in the same fashion. The thermal and mechanical properties were entered as temperature dependent in the analyses. To prevent rigid body motion in the stress analyses, end nodes on the model were constrained so as to approximate the manifold interaction with the testpiece.

RESULTS AND DISCUSSION

The high heat flux encountered by the leading edge of a hypersonic vehicle in flight imposes severe demands on the materials and structures used for these applications. This report describes an experiment and some of the supporting analyses used to evaluate various concepts proposed for this application.

Experimental Conditions

The Hot Gas Test Facility used for this experiment can provide a high enthalpy gas stream with gas total temperatures up to 5600 °F and gas total pressures in the range of 8 to 60 atm. This information is shown in Fig. 2 as an oxygen/hydrogen ratio as a function of the engine combustion chamber pressure. The products of combustion are water vapor and hydrogen for low O/F ratios and water vapor and oxygen for high O/F ratios. The Prandtl number for these mixtures is in the range of 0.6 to 0.8, which is comparable to air. In addition, the ratio of specific heats is in the range of 1.2 to 1.5, which is also comparable to air. Reynolds number similarities can be maintained up to 3.6×10^5 per foot.

The computed (3) stagnation heat flux capability of this experiment is shown in Fig. 8, where the wall temperature is assumed to be constant at 1540 °F. The data are shown as a function of the engine combustion chamber pressure at various approach free-stream Mach numbers. Superimposed on these data are representative heat flux levels for flight Mach numbers ranging from 10 to 24. These data are for comparison purposes only. This shows that, without the shock-on-shock phenomena, the Hot Gas Test Facility can provide a heat flux level of 10 000 Btu/ft^2/sec, which is comparable to flight conditions.

The computed heat flux distribution over the leading edge segment is shown in Fig. 9. This figure shows the characteristically high stagnation heat flux level, which drops rapidly around the cylinder to the level on the downstream portion of the test specimen. The copper crossflow was not designed for this heat flux level. Consequently, the model failed during a test at conditions yielding a stagnation heat flux level between 4000 and 5000 Btu/ft^2/sec.

The experimental procedure was to fire the rocket engine for 3.0 sec and record the transient response of the instrumentation. A typical temperature response of the leading edge is shown in Fig. 10(a). The actual engine firing is about 250 msec after the start of the sequence. Three typical gas temperature histories are shown in fig. 10(b) for shorter firing times of about 1.5 sec. The test specimen temperature rises rapidly and approaches steady state at about 1.5 sec into the sequence. The propellants are shut off at 3.0 sec, and the

temperature decays rapidly. The coolant is flowing during the entire firing sequence. The time constant (time to respond to a change in heat and flux) for the copper test specimen is approximately 0.2 sec.

Temperature Comparisons

Copper and nickel crossflow specimens were tested in a wide range of testing conditions with both water and gaseous hydrogen as coolants. Representative sets of experimental and numerical data for each material and coolant are presented in the following paragraphs. A complete set of the experimental data taken in the Hot Gas Test Facility has been compiled and will be available as a supplement to this paper (1).

Test 31 (RDG 31) consisted of a crossflow water-cooled copper test specimen. Transient temperature and pressure data taken in the test cell are stored on a data acquisition system for later use. Average steady-state temperatures taken from these data and compared with the NASTRAN predictions in Fig. 11 show reasonably good agreement with the predictions, except at the leading edge.

Numerical and experimental temperature comparisons were also made for three additional experiments. The test conditions, together with those of RDG 31, are summarized in Table 1. These comparisons are illustrated in Figs. 12 to 14. These data show relatively good agreement between experimental and calculated temperatures on the copper test specimens. Note that there is a nonsymmetric temperature profile on the finite element model. This was due to a slightly higher pressure distribution on the upper surface of the testpiece during testing, which was taken into consideration for the NASTRAN analysis. Data for the nickel specimens did not show as good an agreement as the copper specimens. This is discussed in the following paragragh.

The RDG 115 and RDG 124 nickel crossflow tests have limited instrumentation, and this accounts for the fewer number of data presented. Figure 14 (RDG 124) does not show as good agreement between measured and predicted data as the data presented for the copper crossflow specimen. Three factors may be contributing to this. First, due to the relatively low thermal conductivity of nickel compared to copper, the resultant thermal gradients are much larger. This makes it more difficult to acquire accurate temperature data with the thermocouples without substantially altering those gradients. Second, examination of the specimen (Fig. 3(b), a photo of the instrumented nickel testpiece after testing) shows an indentation at the center of the leading edge of the panel indicating melting at this spot. Further examination of the figure shows that the hot spot is coincidentally located in line with the outside skin thermocouples. This indicates a hot streak in the gas flow during testing which would result in higher temperatures measured along this line. Note that the analytical predictions in Fig. 14 peak at around 1190 K, which is far below the melting temperature of nickel. Finally, the potential exists for flow separation at the junction of the leading edge semi-cylinder and the downstream flat section. Flow separation and reattachment at this point can lead to higher heat flux than predicted by the boundary layer code.

The difference between a high thermal conductivity (copper) test specimen and a moderate level of thermal conductivity (nickel) is shown in Fig. 15. The measured stagnation point temperature has been normalized with a temperature difference which is proportional to the stagnation region heat flux. All the data shown were recorded at similar test conditions. The normalized temperature (and actual temperature) of the copper test specimen is much lower than that of the nickel test specimen and highlights the more efficient cooling afforded by the high conductivity copper. This phenomenon will permit operation of the copper at higher heat flux conditions or will permit a reduction of the coolant required for an equivalent heat flux condition.

Shown in Fig. 16 is the three-dimensional elastic thermal stress profile on a center portion of the copper crossflow model for RDG 80. This small cross section was taken to avoid looking at the edge effects of the constraints. The stresses shown, being the largest of all of the resultant stresses in the analysis, are the Z component stresses as indicated by the axis on the figure. Intuitively, these stresses are unreasonably high in compression. This indicates yielding at the leading edge of the panel. The bulk of the specimen, behind the leading edge, is at a substantially lower temperature than that at the leading edge and, consequently, acts to restrain the thermal growth of the material in the leading edge. This results in high compressive stresses in that local region.

A nonlinear stress analysis with MARC shows substantial yielding in the leading edge region of the crossflow specimen as shown in Fig. 17. The yield stress for copper was assumed to be 7 ksi in tension and compression. Only half of the model was used because of the intensive CPU requirements for a nonlinear analysis. Time dependent effects will be utilized in the analysis to further investigate the nonlinear behavior of the crossflow specimen.

Two possible ways to reduce the stresses in the leading edge would be either to use a materials with a lower coefficient of thermal expansion or to maintain a more uniform thermal gradient throughout the structure. The latter involves an optimization process and will not be discussed here; however, minimizing the thermal expansion of a material can be accomplished through the use of metal matrix graphite fiber composites. Graphite fiber (P100 type) actually has a negative coefficient of thermal expansion (-0.9×10^{-6}) and when incorporated into a metal matrix can restrain the overall material from large deformation when under thermal load. In addition, certain graphite fibers have a very high thermal conductivity (430 Btu/hr/ft/°F) along the longitudinal direction. However, recent unpublished data have shown the thermal conductivities to be more than an order of magnitude less (5 Btu/hr/ft/°F assumed for analysis purposes) through the transverse direction of the fiber. This could present thermal problems or advantages depending on the application of a

graphite/metal matrix composite. One of the benefits of a thermal/structural program, such as described herein, is to use the advantages and avoid the problems associated with the anisotropy of composites.

CONCLUDING REMARKS

The Hot Gas Test Facility is a good simulation of the high heat flux environment of hypersonic flight up to Mach numbers of 10 to 24. Heat flux levels up to 10 000 Btu/ft^2/sec are attainable at the stagnation line of the leading edge, and this heat flux is comparable with values projected for hypersonic flight (not accounting for shock-on-shock augmentation). In addition, the high enthalpy gas stream has a Prandtl number and specific heat ratio similar to air. However, the aerodynamic phenomena associated with hypersonic flight are not modeled by this facility. Verification of aerothermal load predictions and structural response to large thermal gradients has been initiated with simplified actively cooled cowl lip specimens. Both copper and nickel crossflow models have been tested and analyzed in detail. The predicted model temperatures were generally within acceptable limits of the experimental values.

NASTRAN stress analysis predicted yielding at the leading edge of the crossflow models due to high compressive stresses in that region. This would indicate the need to perform nonlinear analysis of these structures, and this effort has been initiated.

REFERENCES

1. Melis, M.E., Gladden, H.J., Schubert, J.F., Westfall, L.J., and Trimarchi, P.A., 1989, "A Unique Interdisciplinary Research Effort to Support Cowl Lip Technology Development for Hypersonic Applications," NASA TP-2876.
2. Crawford, M.E., and Kays, W.M., 1976, "STAN5—A Program for Numerical Computations of Two-Dimensional Internal and External Boundary Layer Flows," NASA CR-2742.
3. Zukauskas, A., and Ziugzda, J., 1985, Heat Transfer of a Cylinder in Crossflow, Translated by E.I. Bogdanaite, Hewitt, G.F., ed., Hemisphere Publishing Corp., Washington, D.C.
4. Hendricks, R.C., Yeroshenko, V.M., Yaskin, L.A., and Starostin, A.D., 1979, "Bulk Expansion Factors and Density Fluctuations in Heat and Mass Transfer," XV International Congress of Refrigeration, Vol. 2, Paper B1-119.
5. Rohsenow, W.M., and Choi, H.Y., 1961, Heat, Mass and Momentum Transfer, Prentice Hall, Englewood Cliffs, NJ.
6. Crowl, R.J., and Gladden, J.H., 1971, "Methods and Procedures for Evaluating, Forming, and Installing Small-Diameter, Sheathed Thermocouple Wire and Sheathed Thermocouples," NASA TM X-2377.
7. Boyle, R.J., Haas, J.E., and Katsanis, T., 1984, "Comparison Between Measured Turbine Stage Performance and the Predicted Performance Using Quasi-Three-Dimensional Flow and Boundary Analyses," AIAA Paper 84-1299. (NASA TM-83640).

TABLE 1.—SUMMARY OF CROSSFLOW SPECIMEN TESTING

Test number	Material	Oxygen-to-hydrogen (O/F) ratio	Gas temperature, °F	Coolant type	Coolant inlet temperature, °F
RDG 31	Copper	1.55	2666	H_2O	72
RDG 80	Copper	1.65	2800	GH_2	50
RDG 115	Nickel	1.65	2800	H_2O	36
RDG 124	Nickel	1.44	2509	GH_2	48

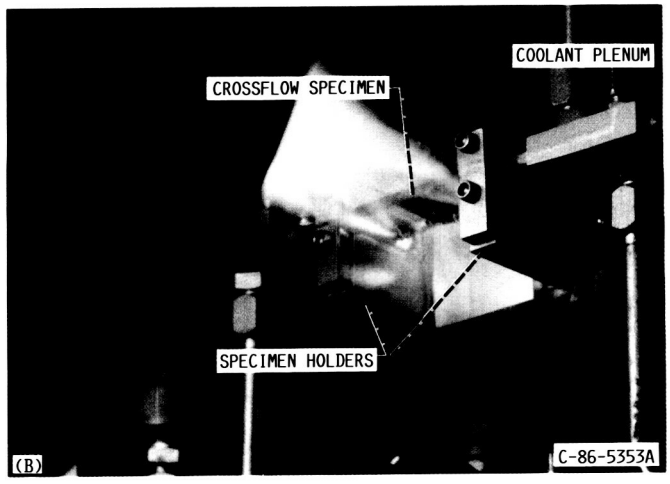

(a) Overall facility view during firing.
(b) Crossflow test specimen mounted in exhaust plume.

Figure 1.—Hot Gas Test Facility.

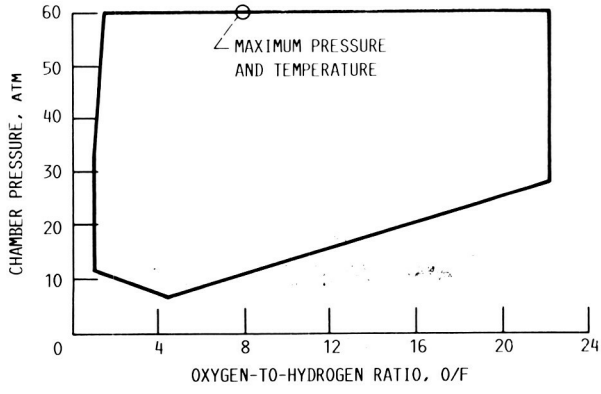

Figure 2.—Hot Gas Test Facility design operating envelope.

ORIGINAL PAGE
COLOR PHOTOGRAPH

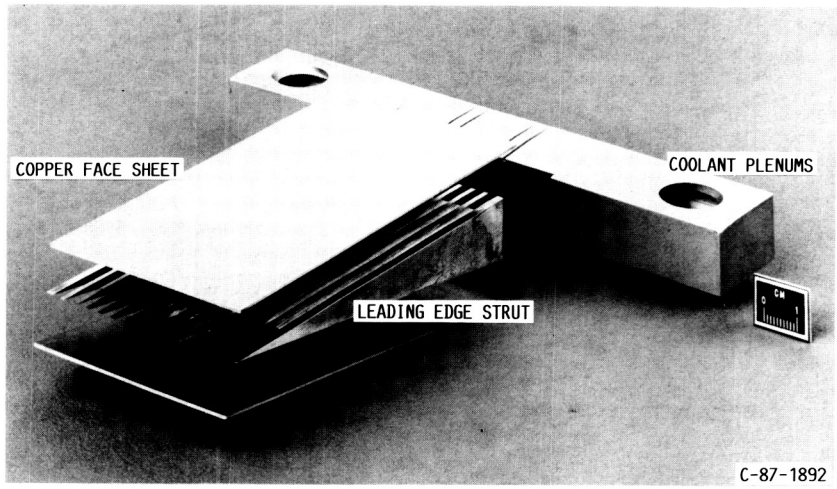

Figure 3.—Exploded view of copper parallel flow model.

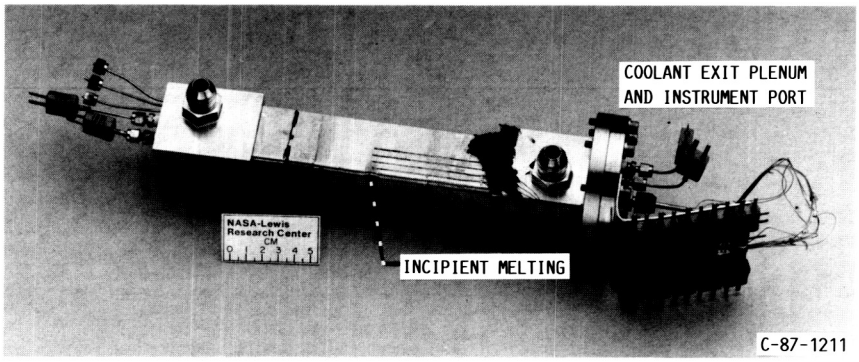

Figure 4.—Assembled and instrumented nickel crossflow model.

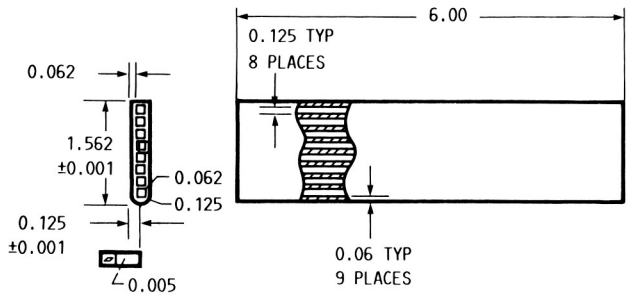

Figure 5.—Schematic illustration of crossflow specimen. (All dimensions are in inches.)

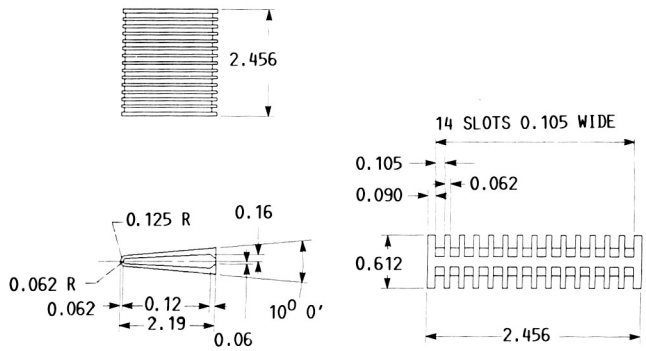

Figure 6.—Schematic illustration of parallel flow specimen. (Linear dimensions are in inches.)

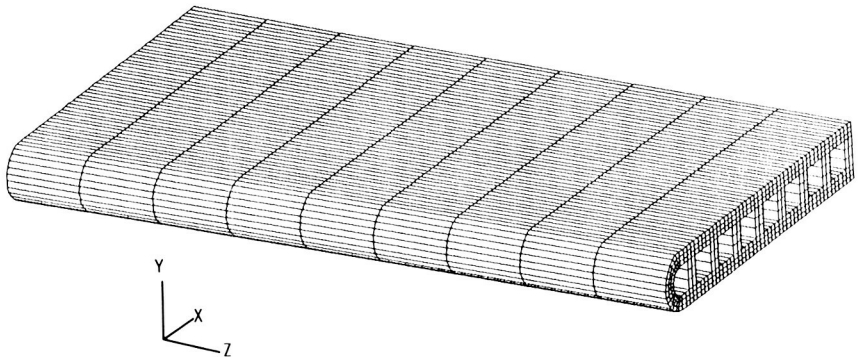

Figure 7.—Crossflow three-dimensional finite element model.

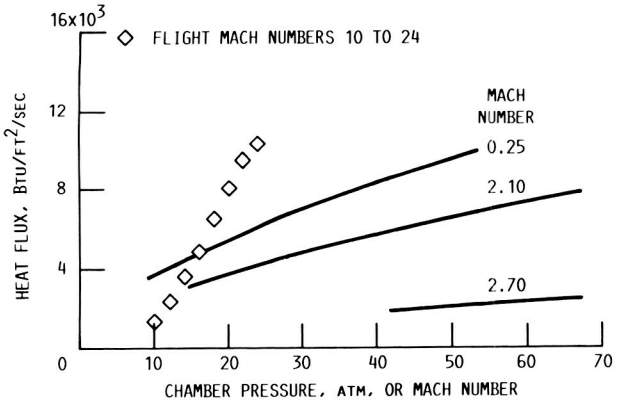

Figure 8.—Computed stagnation heat flux of Hot Gas Test Facility as function of combusion chamber pressure (projected heat flux with flight Mach numbers 10 to 24 shown for comparison; wall temperature, 1540 °F; gas temperature, 5600 °F).

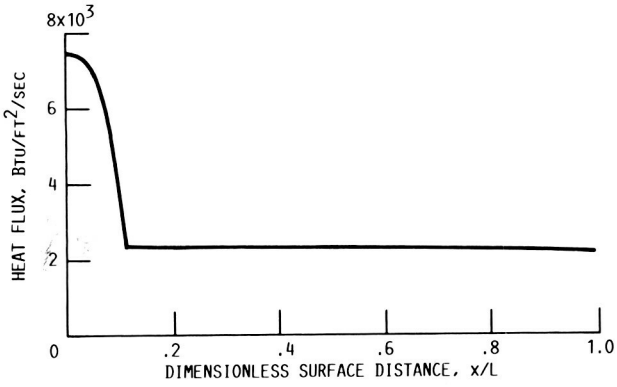

Figure 9.—Computed heat flux distribution over crossflow test specimen at selected test condition (leading edge diameter, 0.25 in.; wall temperature, 1540 °F; gas temperature, 5600 °F; chamber pressure, 13.6 atm).

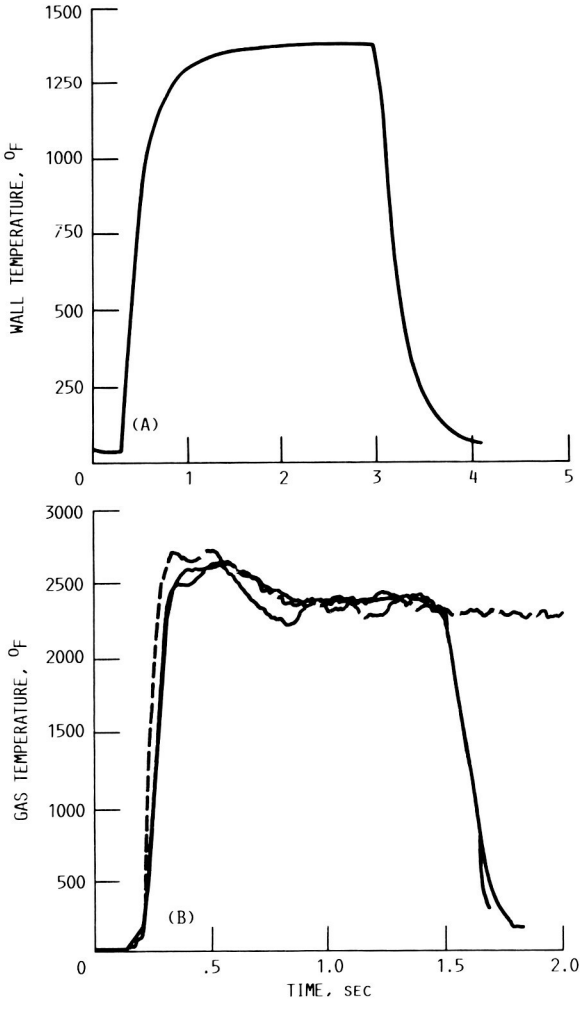

(a) Leading edge temperature of copper crossflow model.
(b) Measured gas temperature histories for three test firings of rocket engine.

Figure 10.—Typical transient temperature data.

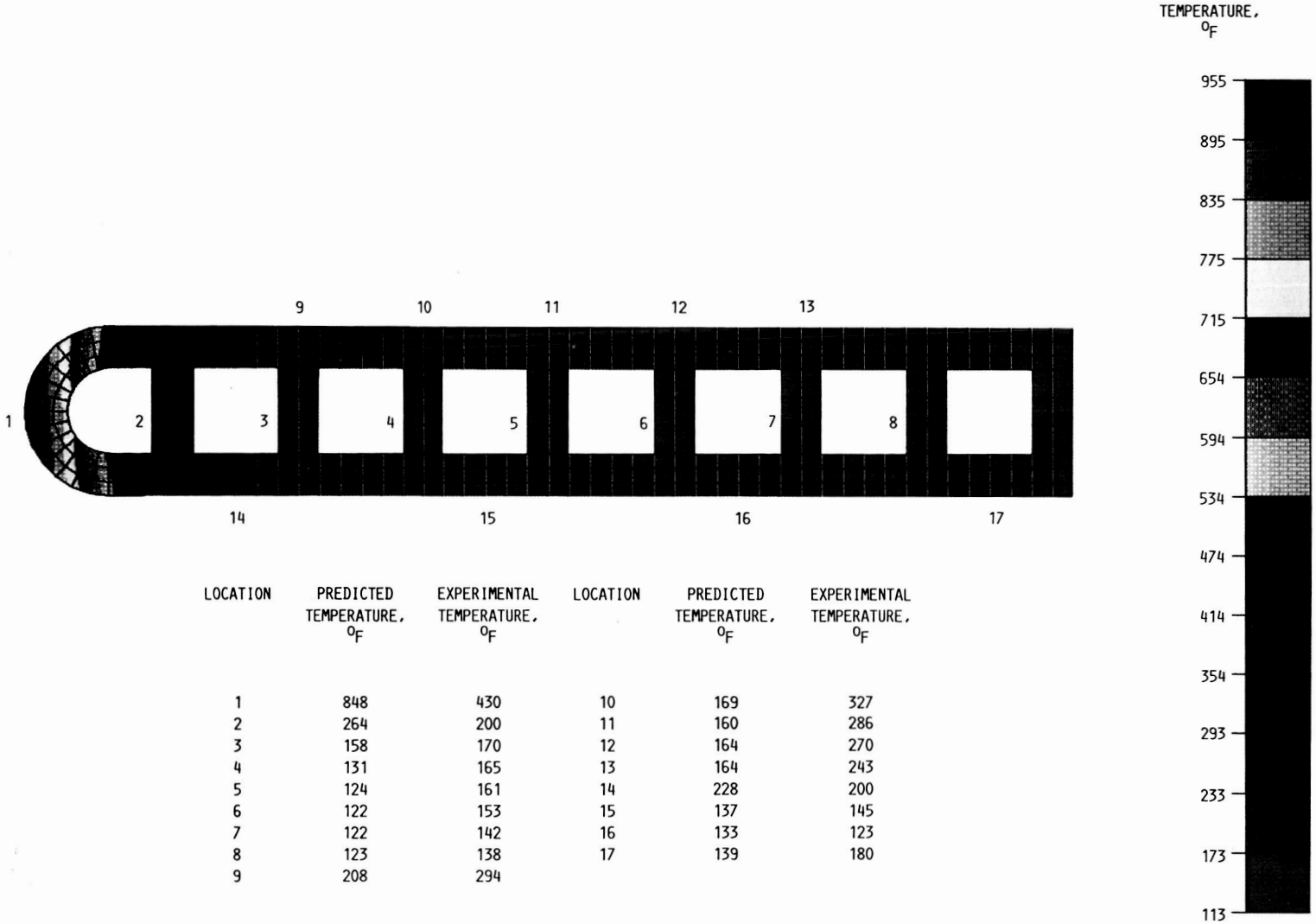

LOCATION	PREDICTED TEMPERATURE, °F	EXPERIMENTAL TEMPERATURE, °F	LOCATION	PREDICTED TEMPERATURE, °F	EXPERIMENTAL TEMPERATURE, °F
1	848	430	10	169	327
2	264	200	11	160	286
3	158	170	12	164	270
4	131	165	13	164	243
5	124	161	14	228	200
6	122	153	15	137	145
7	122	142	16	133	123
8	123	138	17	139	180
9	208	294			

Figure 11.—Comparison of experimental and numerical thermal results of copper crossflow specimen with water coolant.

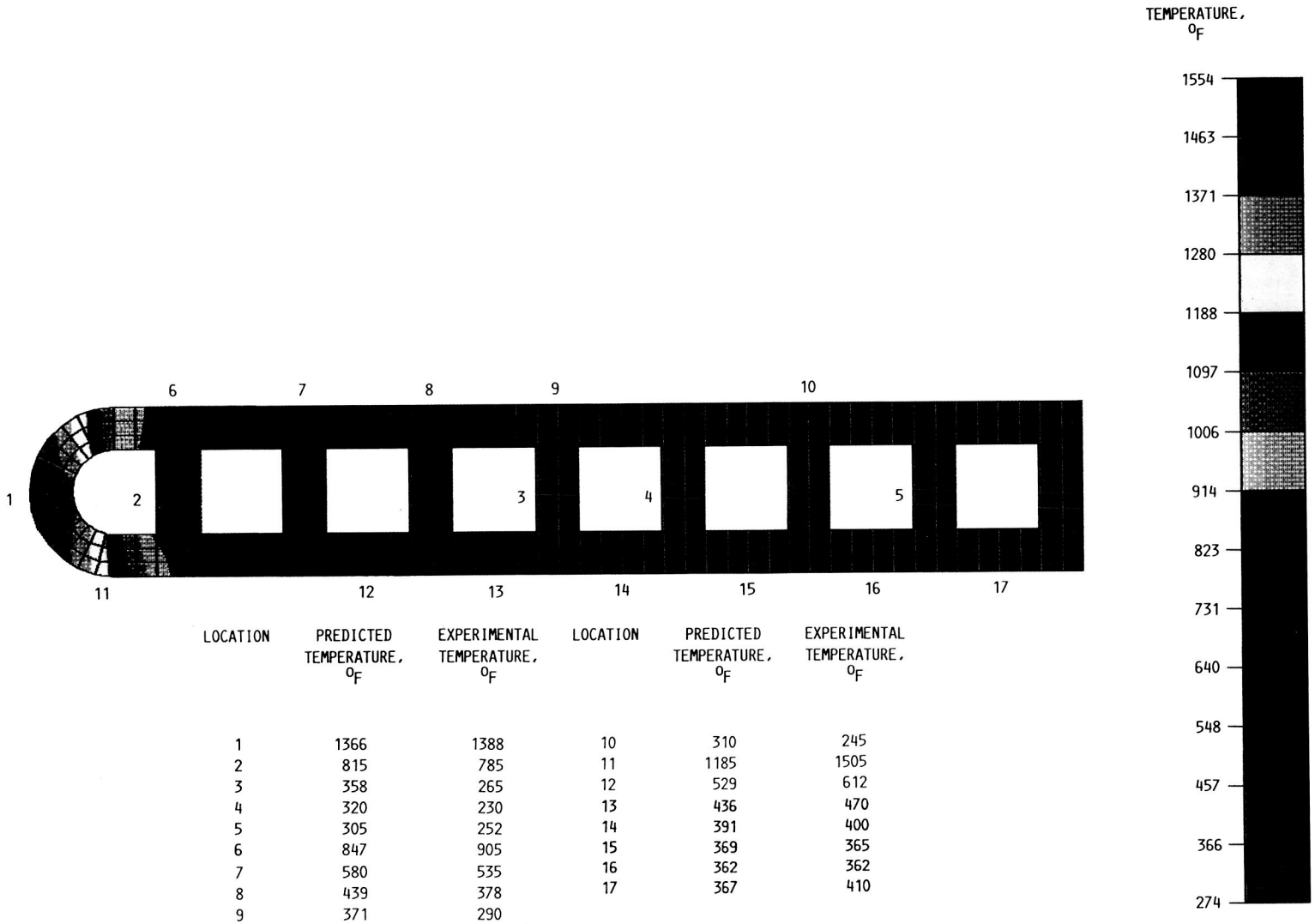

LOCATION	PREDICTED TEMPERATURE, °F	EXPERIMENTAL TEMPERATURE, °F	LOCATION	PREDICTED TEMPERATURE, °F	EXPERIMENTAL TEMPERATURE, °F
1	1366	1388	10	310	245
2	815	785	11	1185	1505
3	358	265	12	529	612
4	320	230	13	436	470
5	305	252	14	391	400
6	847	905	15	369	365
7	580	535	16	362	362
8	439	378	17	367	410
9	371	290			

Figure 12.—Comparison of experimental and numerical thermal results of copper crossflow specimen with gaseous hydrogen coolant.

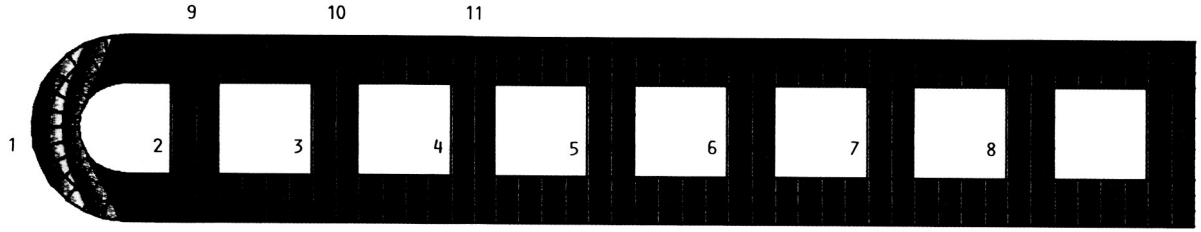

LOCATION	PREDICTED TEMPERATURE, ^{o}F	EXPERIMENTAL TEMPERATURE, ^{o}F	LOCATION	PREDICTED TEMPERATURE, ^{o}F	EXPERIMENTAL TEMPERATURE, ^{o}F
1	1290	1230	7	85	85
2	159	118	8	86	82
3	94	137	9	368	640
4	87	107	10	221	708
5	85	98	11	207	680
6	85	85			

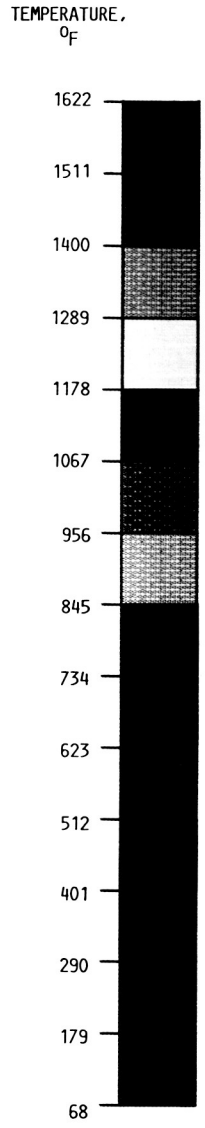

ORIGINAL PAGE
COLOR PHOTOGRAPH

Figure 13.—Comparison of experimental and numerical thermal results of nickel crossflow specimen with water coolant.

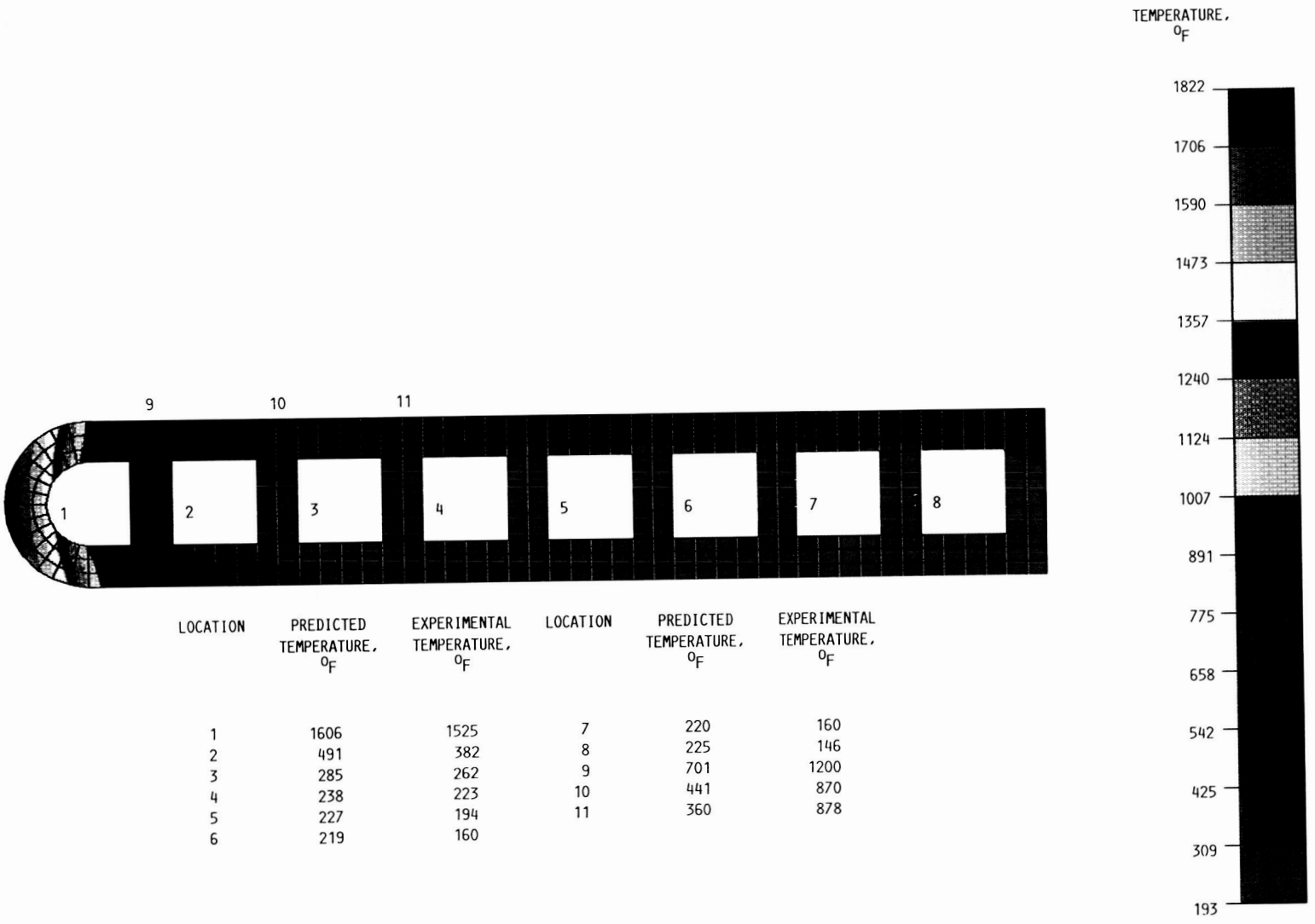

LOCATION	PREDICTED TEMPERATURE, °F	EXPERIMENTAL TEMPERATURE, °F	LOCATION	PREDICTED TEMPERATURE, °F	EXPERIMENTAL TEMPERATURE, °F
1	1606	1525	7	220	160
2	491	382	8	225	146
3	285	262	9	701	1200
4	238	223	10	441	870
5	227	194	11	360	878
6	219	160			

Figure 14.—Comparison of experimental and numerical thermal results of nickel crossflow specimen with gaseous hydrogen coolant.

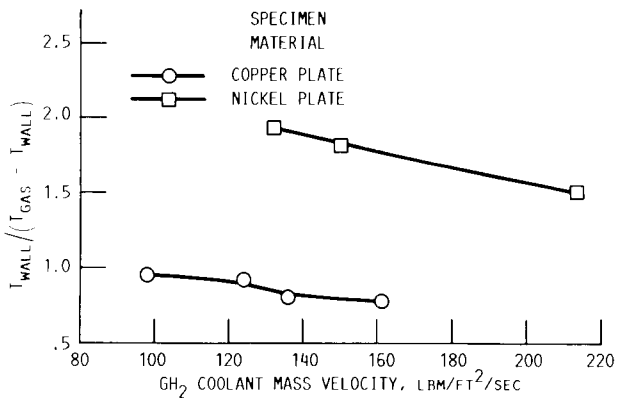

Figure 15.—Comparison of leading edge temperature data taken at similar operating conditions illustrating more efficient cooling of copper model. (T_{WALL} and T_{GAS} are wall temperature and gas temperature, respectively.)

ORIGINAL PAGE
COLOR PHOTOGRAPH

Figure 16.—Three-dimensional elastic thermal stress predictions on copper crossflow specimen.

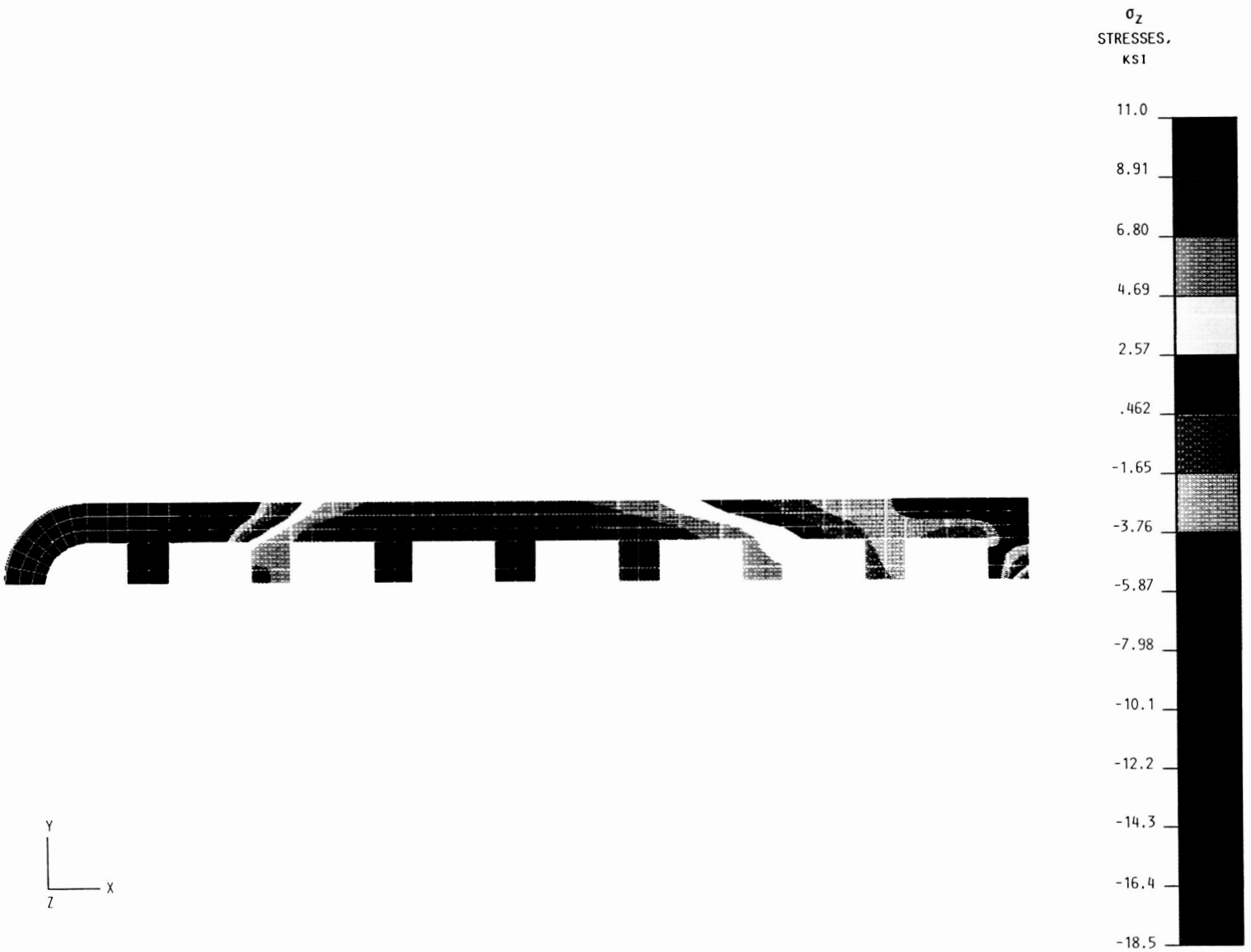

Figure 17.—Three-dimensional elastic/plastic stress predictions on copper crossflow specimen (MARC stress analysis, gaseous hydrogen coolant).

ORIGINAL PAGE
COLOR PHOTOGRAPH

NASA
National Aeronautics and Space Administration

Report Documentation Page

1. Report No.	2. Government Accession No.	3. Recipient's Catalog No.
NASA TM-100931		

4. Title and Subtitle	5. Report Date
A High Heat Flux Experiment for Verification of Thermostructural Analysis	6. Performing Organization Code

7. Author(s)	8. Performing Organization Report No.
Herbert J. Gladden and Matthew E. Melis	E-4202
	10. Work Unit No. 505-63-81

9. Performing Organization Name and Address	11. Contract or Grant No.
National Aeronautics and Space Administration Lewis Research Center Cleveland, Ohio 44135-3191	13. Type of Report and Period Covered Technical Memorandum
12. Sponsoring Agency Name and Address	14. Sponsoring Agency Code
National Aeronautics and Space Administration Washington, D.C. 20546-0001	

15. Supplementary Notes

Prepared for the 1988 Winter Annual Meeting of the American Society of Mechanical Engineers, Chicago, Illinois, November 28—December 2, 1988.

16. Abstract

A major concern in advancing the state-of-the-art technologies for hypersonic vehicles is the development of an aeropropulsion system capable of handling the high heat fluxes during flight. The leading edges of such systems must not only tolerate the maximum heating rates, but must also minimize distortions to the flow field due to excessive blunting and/or thermal warping of the compression surface to achieve the high inlet performance required. A combined analytical and experimental research effort has been established at the NASA Lewis Research Center to study the aerothermodynamic loads on actively cooled structures for hypersonic applications. To address the experimental component of this methodology a hydrogen/oxygen rocket engine has been modified to establish a high enthalpy/high heat flux environment. The facility is capable of providing heat flux levels from about 200 up to 10 000 Btu/ft^2/sec. Crossflow and parallel flow regeneratively cooled models can be tested and analyzed by using cooling fluids of water and hydrogen. In addition, various material types can be tested and compared. These material types include high thermal conductivity copper, nickel, a graphite/copper metal matrix composite, and a tungsten/copper metal matrix composite. This report presents results of the experiment and the characteristics of the Hot Gas Test Facility. The predicted temperature results of the crossflow model are compared with the experimental data on the first monolithic specimens and are found to be in good agreement. Thermal stress analysis results are also presented.

17. Key Words (Suggested by Author(s))	18. Distribution Statement
Heat transfer Stress analysis Leading edge Hydrogen cooling	Unclassified – Unlimited Subject Category 34

19. Security Classif. (of this report)	20. Security Classif. (of this page)	21. No of pages	22. Price*
Unclassified	Unclassified	16	A03

*For sale by the National Technical Information Service, Springfield, Virginia 22161